Preprints of the 21st IFAC World Congress (Virtual)
Berlin, Germany, July 12-17, 2020

Aerodynamic-Efficiency-Constrained Short-Term Frequency Support Control of Wind Turbine Generators

Zhengyang Zhang[*] Zaiyu Chen[*] Guoqiang Yu[**] Tianhai Zhang[**] Minghui Yin[*†] Yun Zou[*]

[*]*School of Automation, Nanjing University of Science and Technology, Nanjing 210094, China (e-mail: njustautozzy@163.com, chenzaiyu1989@gmail.com, ymhui@vip.163.com, zouyun@vip.163.com)*
[**] *Jiangsu Frontier Electric Technology Co. LTD., Nanjing 211102, China (e-mail: guoqiang.yu@163.com, zhangth2009@163.com)*

Abstract: Wind turbine generators (WTGs) can provide short-term frequency support at a frequency event via the stepwise inertial control (SIC) scheme. However, WTGs deviate from the maximum power point tracking (MPPT) operating point when SIC is implemented. A reasonable trade-off between the effectiveness of frequency support and the aerodynamic efficiency of WTGs should be reached in SIC parameters configurations. This paper proposes a modified SIC scheme where the SIC parameters are determined with consideration of wind energy capture losses. Simulation results validate that the proposed scheme improves the system frequency response without causing significant wind energy capture losses.

Keywords: wind turbine generator, stepwise inertial control, wind energy capture efficiency, frequency response, trade-off

1. INTRODUCTION

The past decades have witnessed tremendous increase in the installed capacity of variable-speed wind turbine generators (WTGs). However, at a contingency such as generator tripping, the WTGs inherently cannot respond to system frequency deviation because they are integrated to the grid via power electronic converters (Morren et al., 2006).

The short-term frequency support control enables the WTGs to emulate the inertial response of conventional generators with the kinetic energy stored in the wind rotors (Brisebois et al,. 2011) in order to maintain the frequency stability of power systems that possess high proportion of wind power.

Stepwise inertial control (SIC) is one of the commonly used inertial emulation schemes of WTGs. It modifies the WTGs' electric power reference in a stepwise manner during a frequency event (Ullah et al., 2008; Itani et al., 2011). Several studies have been done on the SIC scheme to improve its adaptability to different operating conditions (Hafiz et al., 2015; Kheshti et al., 2019) or to alleviate the secondary frequency drop when the WTGs are restoring the kinetic energy (Kang et al., 2015; Wu et al., 2016; Yang et al., 2018).

However, when SIC is triggered the WTG is not operated at the optimal speed for maximum power point tracking (MPPT). Consequently, the aerodynamic efficiency of WTGs inevitably declines as the kinetic energy is released.

The effects of SIC parameters on wind energy capture efficiency are investigated in this paper. It is found that a reasonable trade-off between wind energy capture efficiency and frequency support should be reached in the settings of SIC parameters. Otherwise there will be exaggerated wind energy capture losses while the improvement in system frequency response (SFR) is limited.

To this end, this paper proposes a modified SIC scheme where the SIC parameters are determined by solving an optimization model with the constraint of no more than 1% wind energy capture losses. Simulation studies are performed on a WTG-integrated SFR model using MATLAB/Simulink. Simulation results validate that the proposed scheme can avoid excessive wind energy capture losses when providing frequency support.

2. MODELS AND CONTROL SCHEMES

In this section, the mathematical model of a WTG and the principles of SIC are described. Then, an SFR model incorporated with short-term frequency support provided by WTG via SIC is presented.

2.1 WTG Model

The aerodynamic power captured by the wind rotor is expressed as

$$P_m = 0.5\rho\pi R^2 v^3 C_p\left(\lambda, \beta\right) \tag{1}$$

where ρ is air density, R is rotor radius, v is wind speed, $C_p(\lambda,\beta)$ is the power coefficient which is a function of the blade pitch angle β and the tip-speed ratio λ which is defined as

$$\lambda = \frac{\omega_r R}{v} \tag{2}$$

where ω_r is rotor speed (rad/s).

Because this paper is focused on the WTG's operational region between the cut-in and the rated wind speeds, β is fixed at zero

degree and there is an optimal λ_{opt} at which the maximum power coefficient C_{pmax} is yielded.

As illustrated in Fig. 1, the wind rotor is linked to the generator via a gearbox which divides the drive train into the rotor-side low-speed shaft and the generator-side high-speed shaft. Hence, the drive train dynamics can be described by a two-mass model (Boukhezzar et al., 2011), as expressed by

$$\begin{cases} J_r\dot{\omega}_r = T_m - T_{ls} - C_r\omega_r \\ J_g\dot{\omega}_g = T_{hs} - T_g - C_g\omega_g \\ T_{ls} = K_{ls}\left(\theta_r - \theta_{ls}\right) + B_{ls}\left(\omega_r - \omega_{ls}\right) \\ N_g = \omega_g / \omega_{ls} = T_{ls} / T_{hs} \end{cases} \tag{3}$$

where J_r is rotor inertia, J_g is generator inertia, T_{ls} is the low-speed shaft torque, T_{hs} is the high-speed shaft torque, C_r and C_g are respectively the external damping ratios of wind rotor and generator, N_g is the gear ratio, ω_g is generator speed, ω_{ls} is the low-speed shaft speed, θ_r is the rotor-side angular deviation, θ_{ls} is the gearbox-side angular deviation, K_{ls} is the low-speed shaft damping, B_{ls} is the low-speed shaft stiffness, T_m is the aerodynamic torque of wind rotor, T_g is the electromagnetic torque of generator.

Assuming that the low-speed shaft is substantially rigid, the drive train can be simplified to a single lumped model in

$$\begin{cases} J_t\dot{\omega}_r = T_m - T_e = \dfrac{P_m}{\omega_r} - \dfrac{P_e}{\omega_r} \\ J_t = J_r + N_g^2 J_g \end{cases} \tag{4}$$

where T_e is the equivalent generator torque on the low-speed shaft and $T_e = N_g T_g$, P_e is the electric power of generator, J_t is the total inertia of the WTG.

The active power control system of a WTG includes two cascading control loops. The outer-loop sets the active power reference $P_{e,ref}$ for the inner-loop generator controller that adjusts the actual electric power output of generator with the pulse-width modulation strategy. Given that the time scale of electromagnetic response is much smaller than that of the electromechanical response (Boukhezzar et al., 2011), it is assumed that the generator can instantly respond to an assigned $P_{e,ref}$ and $P_e = P_{e,ref}$.

The WTG is usually controlled to maximize wind energy extraction through MPPT strategy (Abdullah et al., 2012) and the corresponding active power reference is expressed by (5).

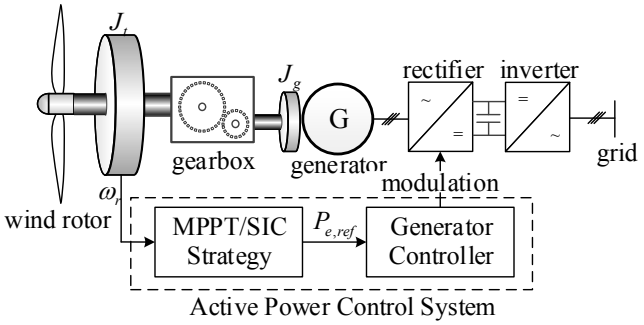

Fig. 1 Block diagram of a WTG

$$P_{e,ref} = 0.5\rho\pi R^5 \frac{C_{p\max}}{\lambda_{opt}^3}\omega_r^3 = K_{opt}\omega_r^3 \tag{5}$$

2.2 SIC Strategy

SIC is triggered when the frequency exceeds its operational limits. As illustrated in Fig. 2, the active power reference of the SIC strategy is determined by a stepwise function (Ullah et al., 2008) that consists of two stages, namely, frequency support and speed recovery.

In the frequency support stage, the WTG temporarily provides additional electric power that mitigates the system power imbalance spurred by the contingency. The corresponding active power reference is $P_{e0}+\Delta P_{up}$ where P_{e0} is the pre-disturbance electric power for MPPT strategy, ΔP_{up} is a constant power surge that enables the release of kinetic energy. The duration of frequency support is T_{up}.

The following speed recovery stage aims at restoring the kinetic energy, during which the electric power is lower than the mechanical power produced by the wind rotor so that the turbine can be accelerated. The corresponding active power reference is $P_{e0}-0.5\Delta P_{up}$. The duration of speed recovery is $2T_{up}$. Once the speed recovery stage is terminated, the MPPT strategy is resumed.

For simplicity, ΔP_{up} and T_{up} are referred to as SIC parameters in the remainder of this paper.

2.3 SIC-Integrated SFR Model

To investigate the frequency dynamics after the activation of SIC, an SFR model (Anderson et al., 1990) incorporated with SIC regulation from WTG is adopted in this paper. As illustrated in Fig. 3, H is the system inertia constant, D is the damping factor, ΔP_C is the power change of conventional generators, K_m, F_H and T_R are parameters of prime mover and governor, R_g is the governor droop, ΔP_W is the power change of WTG, and ΔP_L is the disturbance power.

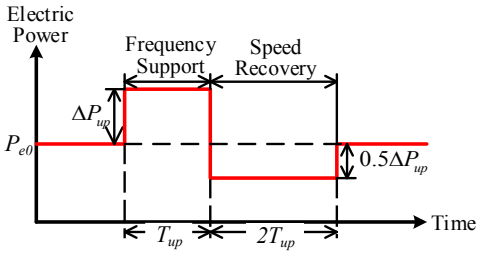

Fig. 2. Active power reference of SIC.

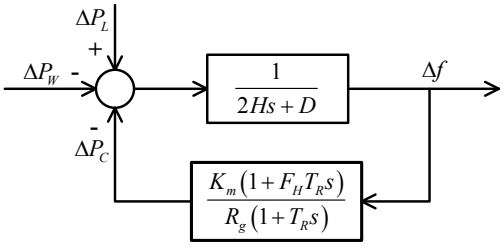

Fig. 3. Block diagram of the SIC-Integrated SFR model.

According to Kheshti et al. (2019), a lower limit is required for the duration of frequency support from SIC in order to ensure the effectiveness of mitigating the maximum frequency deviation $\Delta f_{\max}$ via the power surge of WTG. This limit t_{FN} is calculated by (6) and is the time for frequency deviation to reach $\Delta f_{\max}$ when a step power change with the magnitude of $(\Delta P_{up} - \Delta P_L)$ as input to the SFR model.

$$t_{FN} = \frac{1}{\omega_n \sqrt{1-\xi^2}} \tan^{-1}\left(\frac{\omega_n T_R R_g \sqrt{1-\xi^2}}{\xi \omega_n T_R R_g - 1} \right) \tag{6}$$

where ω_n and ξ are calculated by (7) and (8), respectively.

$$\omega_n = \sqrt{\frac{K_m + DR_g}{2HR_g T_R}} \tag{7}$$

$$\xi = \omega_n \frac{2HR_g + \left(K_m F_H + DR_g\right) T_R}{2\left(K_m + DR_g\right)} \tag{8}$$

In this paper, the $\Delta f_{\max}$ when $T_{up} > t_{FN}$ is interpreted as the expected maximum frequency deviation $\Delta f^*_{\max}$ for a given set of SIC parameters and is determined as

$$\Delta f^*_{\max} = L^{-1}\left[\frac{R_g \omega_n^2 \left(1 + T_R s\right)\left(\Delta P_{up} - \Delta P_L\right)}{s\left(s^2 + 2\xi\omega_n s + \omega_n^2\right)\left(DR_g + K_m\right)} \right]_{t=t_{FN}} \tag{9}$$

where L^{-1} is the inverse Laplace transform operator.

3. IMPACTS OF SIC ON WIND ENERGY CAPTURE EFFICIENCY

WTGs deviate from the MPPT operating point when SIC is implemented, which inevitably impairs wind energy capture efficiency. Effects of SIC parameters on both wind energy capture losses and frequency support are investigated. It is found that a reasonable trade-off between the effectiveness of frequency support and the aerodynamic efficiency of WTGs should be reached in SIC parameters configurations, or there will be excessive wind energy capture losses while no further improvements in frequency support performance can be obtained.

3.1 Wind Energy Capture Losses Caused by SIC

The impacts of SIC on the aerodynamic efficiency of WTG can be quantified by wind energy capture losses (Wang et al., 2015) which is defined as the difference between the ideal wind energy capture and the actual wind energy capture during SIC and is expressed by (10).

$$E_{loss} = \underbrace{\int_{t_0}^{t_0+T_{SIC}} P_m^{MPPT}\, dt}_{E_{cap}^{MPPT}} - \underbrace{\int_{t_0}^{t_0+T_{SIC}} P_m^{SIC}\, dt}_{E_{cap}^{SIC}} \tag{10}$$

where P_m^{SIC} and P_m^{MPPT} are respectively the aerodynamic power produced by the wind rotor under SIC and MPPT strategies, T_{SIC} is the duration of SIC and $T_{SIC}=3T_{up}$, E_{cap}^{MPPT} and E_{cap}^{SIC} are respectively the wind energy captured for MPPT and that for SIC. Considering P_m^{SIC} in (10) is difficult to be measured directly, an estimation expressed by (11) is adopted in this paper to calculate E_{loss}.

$$\hat{P}_m^{SIC} = J_t \omega_r \dot{\omega}_r + P_e^{SIC} \tag{11}$$

where P_e^{SIC} is the electric power of WTG when SIC is implemented.

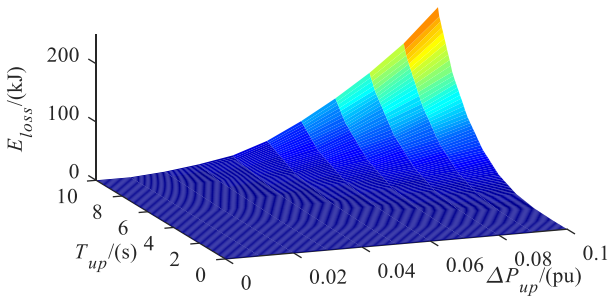

Fig. 4. Wind energy capture losses under different SIC parameters configurations.

3.2 Trade-off between Wind Energy Capture Efficiency and Frequency Support

The short-term frequency support provided by WTGs via SIC is essentially at the cost of the turbine's aerodynamic efficiency. The effects of SIC parameters on both wind energy capture losses and frequency support performance are investigated. It is found that setting too large ΔP_{up} and T_{up} will lead to excessive wind energy capture losses during SIC, while such configurations does not necessarily mean a better frequency support performance.

3.2.1 Effects of SIC Parameters on Wind Energy Capture Losses

According to (10) and (11), for a certain wind speed, E_{loss} determined by the dynamics of rotor speed and the duration of SIC, both are significantly affected by the configurations of SIC parameters. Hence, the effects of SIC parameters on the aerodynamic efficiency should be investigated.

By comparing the E_{loss} for varying ΔP_{up} and T_{up}, it is found that increase in the SIC parameters ΔP_{up} and T_{up} results in higher wind energy capture losses. As shown in Fig. 4:

1) When T_{up} is fixed, E_{loss} rises as ΔP_{up} is increased. The reason is that with larger ΔP_{up}, more kinetic energy is released for the same duration and the further deceleration of rotor speed from its MPPT operating point leads to increasing wind energy capture losses.
2) When ΔP_{up} is fixed, E_{loss} also rises as T_{up} is set longer. Because $T_{SIC}=3T_{up}$, longer T_{up} means that SIC will sustain for a longer period during which the WTG will be operated at non-MPPT speed. As a result, the wind energy capture losses becomes higher.

According to the results analysed above, the aerodynamic efficiency of WTGs will be significantly deteriorated if too large ΔP_{up} and T_{up} are set.

3.2.2 Effects of SIC Parameters on Frequency Support Performance

The performance of frequency support provided by SIC is usually evaluated by the mitigation of both $\Delta f_{\max}$ and the secondary frequency dip (SFD) caused by the termination of frequency support. By investigating the frequency dynamics for different SIC parameters configurations, it is found that the

improvements in SFR is also limited even if very high ΔP_{up} and T_{up} are chosen.

1) Effects of T_{up} on SFR

The frequency dynamics for different values of T_{up} are compared in Fig. 5. It can be seen that when ΔP_{up} is fixed, for $T_{up} \leq 4$s, $\Delta f_{\max}$ gets smaller as T_{up} increases; for $T_{up} > 4$s, FN remains the same though T_{up} increases further. These results can be interpreted as follows.

Smaller T_{up} means earlier withdrawal of the supportive power provided by WTG, which is unfavourable to balancing system active power in the early stage of a contingency and $\Delta f_{\max}$ will be deteriorated (Kheshti et al., 2019). However, once $T_{up} > t_{FN}$, $\Delta f_{\max}$ equals to $\Delta f^*_{\max}$ which is irrelevant to T_{up}, thus increasing T_{up} has nothing to do with reducing $\Delta f_{\max}$. Therefore, T_{up} should be larger than t_{FN} but a too large value for T_{up} is dispensable.

2) Effects of ΔP_{up} on SFR

The frequency dynamics for different values of ΔP_{up} are compared in Fig. 6. It can be seen that when T_{up} is fixed and $T_{up} > t_{FN}$, the larger ΔP_{up} is, the smaller $\Delta f_{\max}$ is but the severer SFD is. These results can be interpreted as follows.

When $T_{up} > t_{FN}$, $\Delta f_{\max}$ equals to $\Delta f^*_{\max}$ which is proportional to ΔP_{up}. Hence, larger ΔP_{up} is favourable to mitigating $\Delta f_{\max}$. On the other hand, because the magnitude of the sudden $1.5\Delta P_{up}$ power drop when WTG terminating frequency support increases as ΔP_{up} gets larger, the system will experience a more significant step disturbance and the SFD worsens. Therefore, the overall SFR may not be improved if ΔP_{up} is too large.

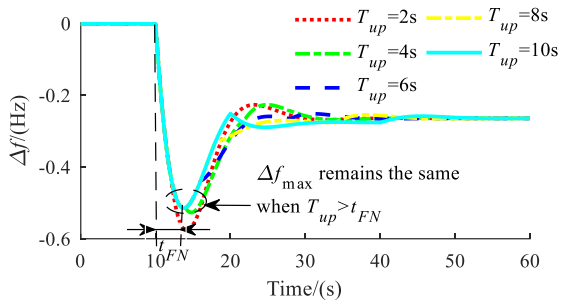

Fig. 5. System frequency response with different T_{up} and same ΔP_{up} (ΔP_{up} =0.05 pu).

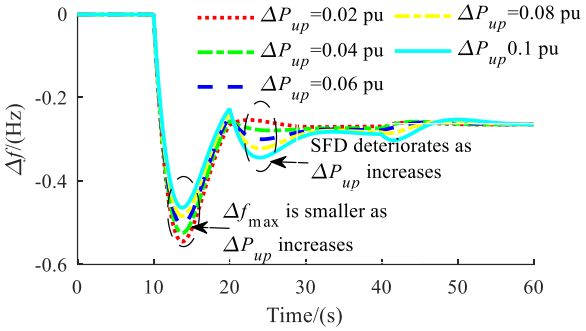

Fig. 6. System frequency response with different ΔP_{up} and same ΔP_{up} (T_{up} =10 s).

According to the above analyses, a reasonable trade-off between the effectiveness of frequency support and the aerodynamic efficiency of WTGs should be reached in SIC parameters configurations, so that the frequency response can be improved at a lower cost of wind energy capture losses.

4. PROPOSED WIND ENERGY CAPTURE EFFICIENCY CONSTRAINED SIC SCHEME

A modified SIC scheme is proposed in order to achieve a reasonable trade-off between wind energy capture efficiency and frequency support. In the proposed scheme, SIC parameters are determined by solving an optimization model constrained by wind energy capture losses.

4.1 SIC Parameters Optimization Model

Decision variables of the SIC parameters optimization model are ΔP_{up} and T_{up}. The objective function and constraints are described as follows. Because the concept of SIC strategy aims at providing short-term frequency support at a contingency, minimizing frequency deviation, especially the nadir, is of top priority. Hence, the objective of optimizing SIC parameters is to minimize the expected maximum frequency deviation for a given set of SIC parameters, as expressed by (12).

$$\min \left| \Delta f^*_{\max} \right| \tag{12}$$

To prevent excessive wind energy capture losses, the wind energy capture losses during SIC is limited to certain percentage of the wind energy captured for MPPT, as expressed by (13).

$$E_{loss} < \varepsilon \underbrace{\int_{t_0}^{t_0+T_{SIC}} P_m^{MPPT} dt}_{E_{cap}^{MPPT}} \tag{13}$$

The limit ε can be varied according to wind power penetration level, contingency scale, and wind condition. In this paper, ε is set as 1%.

Considering that a too early frequency support termination may induce unexpected deterioration of $\Delta f_{\max}$, the constraint (14) is utilized to guarantee that $\Delta f^*_{\max}$ can be reached so as to be minimized in (12).

$$T_{up} > t_{FN} \tag{14}$$

In case the SFD occurring at the end of the frequency support stage exceeds the frequency nadir, the frequency deviation when $t > t_{FN}$ should be smaller than the minimized $\Delta f^*_{\max}$, as expressed by (15).

$$\left| \Delta f_{t>t_{FN}} \left(t, \Delta P_{up}, T_{up} \right) \right| < \left| \Delta f^*_{\max} \right| \tag{15}$$

By combining the objective function (12) and the constraints (13), (14), and (15), the proposed SIC parameters optimization model is obtained.

4.2 Model Solution

According to 4.1, both the WTG and the system frequency dynamics are required to solve the SIC parameters optimization model. Given the nonlinearities in the WTG integrated SFR model, the Genetic Algorithm (GA) is adopted to optimize the SIC parameters for its high efficiency and capability of searching global solutions for nonlinear and nonconvex optimization problems (Goldberg 1989).

Flowchart of the SIC parameters optimization based on GA is illustrated in Fig. 7.

5. SIMULATION VALIDATION

In this section, simulation studies are performed to validate the effectiveness of the proposed SIC scheme.

5.1 Simulation Configurations

A WTG-integrated SFR model is established in MATLAB/Simulink for simulation validation. The WTG is modelled as the three-bladed Controls Advanced Research Turbine (CART3) (Wright et al., 2008) using the fatigue, aerodynamics, structures and turbulence (FAST) module (Jonkman et al., 2005) developed by the National Renewable Energy Laboratory (NREL). Key parameters of the CART3 turbine are listed in Table 1. System frequency response is obtained by the SFR model described in section 2.3 and the relevant specifications of the SFR model (Anderson et al., 1990) are shown in Table 2.

The simulation scenario is set as follows. The wind speed for WTG is 10 m/s. The wind power penetration level is 10%. The frequency event is set as a 0.1 pu step increase in load at t=10s.

5.2 SIC Parameters Optimization

Both the proposed SIC scheme and the conventional one (Ullah et al., 2008) are respectively applied on the WTG for comparative analysis. SIC parameters of the conventional scheme are also optimized based on the optimization model presented in 4.1 but the constraint for wind energy capture losses is excluded.

The SIC parameters optimizations are done by the GA solver embedded in the MATLAB optimization toolbox. Configurations of the GA solver are shown in Table 3. The optimization is terminated if either of the following conditions is satisfied: 1) variation in the best fitness value over 200 consecutive generations is less than 1×10^{-6}; 2) the number of iteration reaches 500.

Optimization results of SIC parameters are shown in Table 4 and the corresponding WTG electric power of the proposed and the conventional SIC schemes are shown in Fig. 8.

5.3 Simulation Results

Simulation results of the proposed and the conventional SIC scheme are compared from the following two aspects.

1） Wind energy capture losses

E_{loss} of the proposed and the conventional SIC schemes are shown in Table 4. Compared with the conventional scheme, the wind energy capture losses of the proposed SIC scheme is reduced by 63.56% and is within the predetermined limit which is 1% of the wind energy captured for MPPT. These results indicate that the proposed SIC scheme can prevent excessive wind energy capture losses by imposing the constraint (13) on SIC parameters optimization.

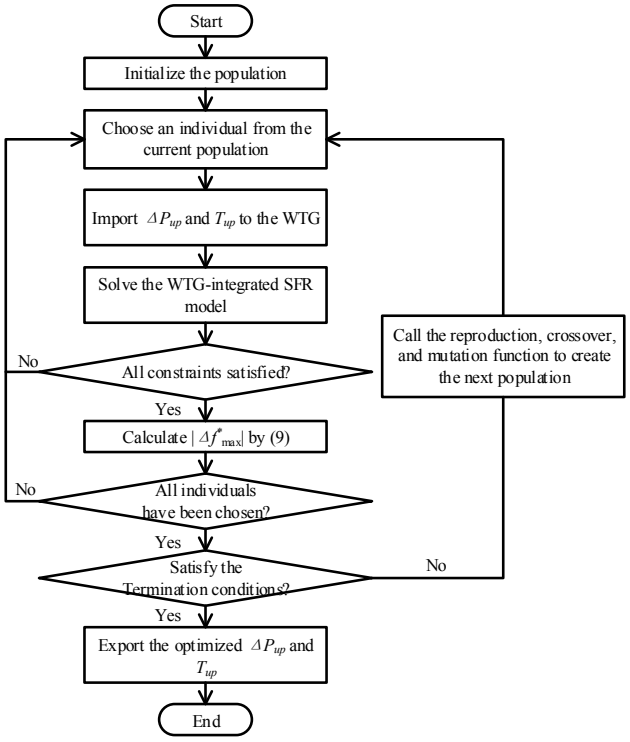

Fig. 7. Flowchart of the GA-based optimization.

Table 1. Parameters of the CART3 turbine.

Parameters (Units)	Values
rated power (kW)	600
ρ (kg·m^3)	1.225
R (m)	20
rotor inertia (kg·m^2)	5.492×10^5
C_{pmax}	0.4603
λ_{opt}	5.8

Table 2. Parameters of the SFR model.

Parameters (Units)	Values
H (s)	8
D	0
K_m	0.95
F_h	0.3
T_r (s)	8
R_g	0.05

Table 3. Configurations of the GA solver

Options	Settings
population size	100
selection function	stochastic uniform
crossover function	scattered
mutation function	gaussian
scaling function	rank
elite count	10
crossover fraction	0.8

2） System frequency response

Frequency dynamics for the proposed and the conventional SIC schemes are shown in Fig. 9. Compared with the baseline case where only MPPT strategy is implemented, both the proposed and the conventional SIC schemes improve the frequency nadir by 0.09 Hz while no severe SFD is observed.

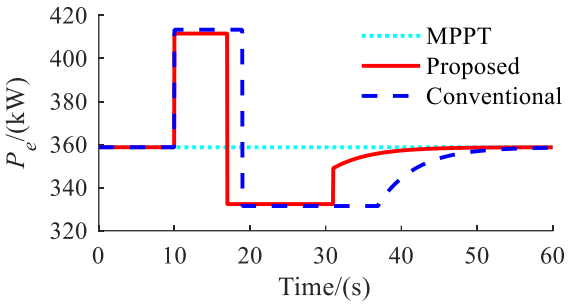

Fig. 8. Simulation results of the electric power of the WTG.

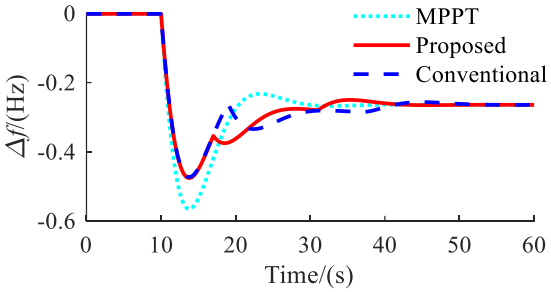

Fig. 9. Simulation results of system frequency response.

Table 4. Optimization results of SIC parameters and simulation results of $E_{loss}$and E_{cap}^{MPPT}

SIC scheme	ΔP_{up} (kW)	T_{up} (s)	E_{loss} (kJ)	E_{cap}^{MPPT} (kJ)
Proposed	52.86	7	47.23	7534
Conventional	54.72	9	129.6	9687

These results show that frequency support performance of the proposed SIC scheme is similar to that of the conventional scheme.

It can be summarized from the above results that the proposed SIC scheme can achieve the expected frequency response performance at a reduced cost of wind energy capture losses.

6. CONCLUSIONS

An SIC scheme is proposed to achieve the trade-off between wind energy capture efficiency and frequency support performance. SIC parameters of the proposed scheme are optimized with the constraint of wind energy capture losses. Simulation results validate that the proposed SIC scheme is capable of improving the frequency response while limiting the wind energy capture losses. It should be pointed out that in this paper the wind speed is assumed to be constant. Nevertheless, in practice the WTGs are operated under complex turbulent wind conditions. Further researches should be conducted to design the SIC parameters that coordinate frequency support and wind energy capture under varying wind speeds.

ACKNOWLEDGEMENTS

This work is supported by the National Natural Science Foundation of China (61673213, 61773214, 51977111) and the Science and Technology Project of Jiangsu Frontier Electric Technology Co. LTD “Research and Application of Primary Frequency Regulation Control System for grid-connected Wind Turbines”.

REFERENCES

Anderson, P. M. and Mirheydar, M. (1990). A low-order system frequency response model. *IEEE Trans. Power Syst.*, 5(3), 720-729.

Abdullah, M. A., Yatim, A. H., Tan, C. W., and Saidur, R. (2012). A review of maximum power point tracking algorithms for wind energy systems. *Renew. Sust. Energ. Rev.*, 16(5), 3220-3227.

Brisebois, J. and Aubut, N. (2011). Wind farm inertia emulation to fulfil Hydro-Québec's specific need. In *2011 IEEE Power and Energy Society General Meeting*, Detroit, MI, USA

Boukhezzar, B. and Siguerdidjane, H. (2011). Nonlinear control of a variable-speed wind turbine using a two-mass model. *IEEE Trans. Energy Convers.*, 26(1), 149-162.

Goldberg, D. E. (1989). Genetic Algorithms in Search, Optimization, and Machine Learning. MA: Addison-Wesley.

Hafiz, F. and Abdennour, A. (2015). Optimal use of kinetic energy for the inertial support from variable speed wind turbines. *Renew. Energy*, 80, 629-643.

Itani, S. El, Annakkage, U. D., Joos G. (2011). Short-term frequency support utilizing inertial response of DFIG wind turbines. In *2011 IEEE Power and Energy Society General Meeting*, Detroit, MI, USA.

Jonkman, J. M. and Buhl, M. L. Jr. (2005). FAST user's guide. National Renewable Energy Laboratory, Golden, CO.

Kang, M., Lee, J., Hur, K., Park, S. H., Choy, Y., and Kang, Y. C. (2015). Stepwise inertial control of a doubly-fed induction generator to prevent a second frequency dip. J. *Electr. Eng. Technol.*, 10(76), 2221-2227.

Kheshti, M., Ding, L., Bao, W., Yin, M., Wu, Q., Terzija, V. (2019). Toward Intelligent Inertial Frequency Participation of Wind Farms for the Grid Frequency Control. *IEEE Trans. Ind. Inform.*, Early Access.

Morren, J., Pierik, J., W. H. de Haan, S., (2006). Inertial response of variable speed wind turbines. *Electr. Power Syst. Res.*, 76, 980-987.

Ullah, N. R., Thiringer, T., and Karlsson, D. (2008). Temporary primary frequency control support by variable speed wind turbines—potential and applications. *IEEE Trans. Power Syst.*, 23(2), 601-612.

Wang, H., Chen, Z., and Jiang, Q. (2015). Optimal control method for wind farm to support temporary primary frequency control with minimised wind energy cost. *IET Renew. Power Gener.*, 9(4), 350-359.

Wu, Z., Gao, W., Wang, X., Kang, M., Hwang, M., Kang, Y. C., Gevogian, V., and Muljadi, E. (2016). Improved inertial control for permanent magnet synchronous generator wind turbine generators. *IET Renew. Power Gener.*, 10(9), 1366-1373.

Wright, A. D. and Fingersh, L. J. (2008). Advanced control design for wind turbines—Part I: Control design, implementation, and initial tests. Technical Report NREL/TP-500-42437. National Renewable Energy Laboratory, Golden, CO.

Yang, D., Kim, J., Kang, Y. C., Muljadi, E., Zhang, N., Hong, J., Song, S-H., Zheng, T. (2018). Temporary Frequency Support of a DFIG for High Wind Power Penetration. *IEEE Trans. Power Syst.*, 33(3), 3428-3437.